

Lattice dynamics of the high- T_c superconductor $\text{YBa}_2\text{Cu}_3\text{O}_{7-x}$

W. Kress

*Max-Planck-Institut für Festkörperforschung, Postfach 80 06 65, D-7000 Stuttgart 80,
Federal Republic of Germany*

U. Schröder

Universität Regensburg, D-8400 Regensburg, Federal Republic of Germany

J. Prade,* A. D. Kulkarni, and F. W. de Wette

Physics Department, University of Texas, Austin, Texas 78712

(Received 11 April 1988)

We present a lattice-dynamical calculation of the phonon dispersion curves and the one-phonon density of states of the high- T_c superconductor $\text{YBa}_2\text{Cu}_3\text{O}_{7-x}$ in the framework of a shell model, which is based on a short-range overlap and long-range Coulomb potentials. The parameters of these potentials are obtained from best fits to the measured phonon dispersion curves of BaTiO_3 and appropriate metal oxides. The model for $\text{YBa}_2\text{Cu}_3\text{O}_{7-x}$ so obtained leads to rather satisfactory agreement with the available ir and Raman data without any major adjustments of the potential parameters. These results thus provide a solid basis for the discussion of the role of phonons for the high transition temperature and a guide for further experimental studies of the vibrational properties of this and related compounds.

The discovery of the high superconducting transition of the La-Ba-Cu-O system by Bednorz and Müller¹ has caused unprecedented worldwide activities in the search and characterization of high- T_c materials. One of the promising new materials with a T_c of about 90 K is $\text{YBa}_2\text{Cu}_3\text{O}_{7-x}$ which has first been investigated by Chu *et al.*² and has since then been studied by many experimental groups using a variety of techniques. So far neither the experimental investigations nor the many theoretical attempts have clearly revealed the microscopic pairing mechanism which leads to the high transition temperatures. Even if the electron-phonon coupling alone would be insufficient to explain the high transition temperatures and other mechanisms would also come into play, it could well be that the phonon contribution still makes up a significant part of T_c in these compounds. To contribute to this discussion we focus in this paper on the calculation of the lattice vibrations and their spectra. So far the experimental studies of the lattice vibrations of $\text{YBa}_2\text{Cu}_3\text{O}_{7-x}$ have been restricted to infrared (ir) and Raman-scattering studies, i.e., to phonons of small wave vectors, since single crystals of sufficient size are not yet available to perform inelastic neutron-scattering measurements which would reveal the full dispersion curves. The precise knowledge of the zone-boundary phonons is, however, indispensable for the investigation of the electron-phonon coupling contribution to T_c , since these phonons give rise to important features in the phonon density of states $g(\omega)$, which enters the Eliashberg equations. In this paper, we present a full calculation of the lattice vibrations of $\text{YBa}_2\text{Cu}_3\text{O}_{7-x}$ in the framework of a shell model, based on interatomic short- and long-range potentials. The results are presented in the form of phonon dispersion curves and the phonon density of states.

Calculations. The large number of particles per unit cell in combination with the deviation from the full cubic

symmetry leads in $\text{YBa}_2\text{Cu}_3\text{O}_{7-x}$ to a large number of yet unknown force constants, which would have to be determined from experimental data before we could calculate the phonon dispersion curves if we would proceed in the way most model calculations are performed in the literature. Since experimental information about the phonon dispersion curves is very limited and essentially restricted to the long-wavelength data obtained from ir and Raman-scattering measurements, we have to adopt a different procedure here. This procedure has the additional advantage that it gives a better insight into the underlying physics. Instead of starting from the force constants, we base our calculations on interaction potentials which we decompose into a short-range overlap part, for which we assume a Born-Mayer-type potential, and a long-range part with a Coulomb potential. In addition, we treat the displacement-induced deformations of the electronic charge density in the framework of a shell model. The first step is the determination of the pair potentials. For ions with electronic closed-shell configurations such as perovskites and alkali halides, these pair potentials are to a large extent independent of the spatial arrangement of the ions in the crystal. In fact, the pair potentials of fluoridic perovskites are very similar to those of alkali halides³ and in these compounds bulk potentials can be carried over to the surface and continue to provide realistic force constants even though the local symmetry has changed quite drastically and the distances of the interacting ions have changed due to surface relaxation.^{4,5} Because of this, and the fact that the $\text{YBa}_2\text{Cu}_3\text{O}_{7-x}$ structure has certain similarities with the perovskite structure, we will obtain the short-range pair potentials for $\text{YBa}_2\text{Cu}_3\text{O}_{7-x}$ from known potentials of perovskites and metal oxides with rock-salt structure which contain the same ion pairs as $\text{YBa}_2\text{Cu}_3\text{O}_{7-x}$, or at least ion pairs for which we have good reasons to expect that the interaction

potentials are nearly the same as those of the related ion pairs in $\text{YBa}_2\text{Cu}_3\text{O}_{7-x}$. We point out that these structural similarities with the perovskites are even more pronounced for the original high- T_c compound $\text{La}_{2-x}\text{Ba}_x\text{CuO}_4$. As in certain perovskites, the interplay of structure and interactions⁶ in $\text{La}_{2-x}\text{Ba}_x\text{CuO}_4$ can lead to phonon instabilities due to a critical cancellation of short-range overlap and long-range Coulomb forces (manifested in the tetragonal-to-orthorhombic transition of $\text{La}_{2-x}\text{Ba}_x\text{CuO}_4$). Therefore, the inclusion and careful treatment of both types of forces is absolutely essential.

As mentioned, the short-range interactions between neighboring ions are represented by Born-Mayer potentials:

$$V_{ij}(r) = a_{ij} \exp(-b_{ij}r), \quad (1)$$

where i, j label the ions and r is their distance. We take into account short-range interactions between Cu and O, Ba and O, Y and O, and between neighboring oxygen atoms. Although the Cu-O distance is different for different Cu-O pairs in the $\text{YBa}_2\text{Cu}_3\text{O}_{7-x}$ structure, and in consequence leads to different sets of force constants for different Cu-O pairs, these force constants arise in our model from two closely related Born-Mayer potentials which, in fact, are characterized by just three parameters (cf. Table I). The physical reason for the slight difference between the Cu(1)-O and Cu(2)-O potentials is that the Cu-O pairs are in different crystal environments, resulting in different hybridization of their electronic states. The advantage of using short-range potentials (rather than force constants) is that, in spite of having 13 particles in the unit cell, the number of short-range parameters is only 9.

We determine the parameters a_{ij} and b_{ij} of our pair potentials as well as the parameters Y_i and k_i which determine the electronic polarizabilities from fits to the measured phonon dispersion curves of related compounds. From BaTiO_3 (Refs. 7 and 8) we obtain the O-O and Ba-O potentials and the parameters Y_i and k_i of Ba and O. The Cu-O potential and the Y_i and k_i of Cu we take from NiO ,⁹ since we believe that the short-range overlap potentials of Cu-O and Ni-O are very similar. Finally, we take the corresponding Y-O parameters from SrO ,¹⁰ since Y and Sr have roughly the same ionic radii. For the ionic

charges, we initially choose the nominal values +3, +2, +2, for Y, Ba, and Cu, respectively. The charge of the oxygen ions is then determined by the required charge neutrality of the unit cell.

The procedure just described gave a set of starting values of the model parameters for the lattice-dynamical calculations. These parameters were then given small further adjustments to give stable dynamics, i.e., real phonon frequencies over the entire Brillouin zone (BZ). The parameters for the model $\text{YBa}_2\text{Cu}_3\text{O}_{7-x}$ are listed in Table I, where we list for comparison, in addition to the Born-Mayer constants a_{ij} and b_{ij} , some radial and tangential force constants A_{ij} and B_{ij} , which follow from the Born-Mayer potentials (1), as follows:

$$\begin{aligned} A_{ij} \left[\frac{e^2}{2v_a} \right] &= \frac{d^2}{dr^2} V_{ij}(r) \Big|_{r=r_{ij}^0}, \\ B_{ij} \left[\frac{e^2}{2v_a} \right] &= \frac{1}{r} \frac{d}{dr} V_{ij}(r) \Big|_{r=r_{ij}^0}, \end{aligned} \quad (2)$$

where e is the electronic charge, v_a the volume of the unit cell, and r_{ij}^0 the equilibrium distance of ions i and j . We have ordered these selected A, B pairs according to decreasing values to bring out the hierarchy of the various ion pairs; it is strongest for Cu(2)-O and weakest for O-O.

The high- T_c compound $\text{YBa}_2\text{Cu}_3\text{O}_{7-x}$ does not undergo a structural phase transition between 10 K and 298 K. Therefore, we choose for our calculations the crystal structure of the annealed room-temperature sample as determined by Beech, Miraglia, Santoro, and Roth¹¹ (structure no. 3). The absence of a transition implies that we do not expect $\text{YBa}_2\text{Cu}_3\text{O}_{7-x}$ to exhibit a pronounced soft-mode behavior at the zone boundary, as was found for the $\text{La}_{2-x}\text{M}_x\text{CuO}_4$ compounds.⁶

When we compare the calculated phonon frequencies at the zone center with the ir and Raman data^{12,13} we find a reasonable agreement for all modes except the A_g mode seen in Raman scattering at 435 cm^{-1} , which in our first calculations was found above 620 cm^{-1} . In this mode, a uniformly charged O(II)-O(III) plane moves rigidly with respect to a Cu plane and the Coulomb interactions between these two planes obviously causes the high frequency. We were able to lower this mode to 373 cm^{-1}

TABLE I. Parameters of the model: a, b : Born-Mayer constants; Z, Y, k : ionic charge, shell charge, and on-site core-shell force constant of the ion (v_a : volume of the unit cell); A, B : radial and tangential force constants between the ions for selected ion pairs, in order of decreasing strengths to bring out the hierarchy of interaction strengths. For the labeling of Cu and O ions, we refer to Ref. 11.

Interaction	a (eV)	b (\AA^{-1})	Ion	Z ($ e $)	Y ($ e $)	k (e^2/v_a)	Interaction	A [$e^2/(2v_a)$]	B [$e^2/(2v_a)$]
Y-O	3010	2.90	Y	2.85	-1.42	872	Cu(2)-O(II)	576	-90.8
Ba-O	3225	2.90	Ba	1.90	2.32	165	Y-O(II)	563	-80.5
Cu(1)-O	1260	3.45	Cu(1)	2.00	3.22	1000	Ba-O(II)	114	-13.2
Cu(2)-O	1260	3.29	Cu(2)	2.00	3.22	1000	O(III)-O(II)	62	-7.5
O-O	1000	3.00	O(II), O(III)	-1.81	-2.70	252			
			O(I), O(IV)	-1.81	-2.70	252 (k_{\parallel}) ^a			
						1675 (k_{\perp}) ^a			

^aFor O(I) and O(IV) we assume anisotropic polarizability with force constants k_{\parallel} (parallel to the Cu-O directions) and k_{\perp} (perpendicular to the Cu-O directions).

TABLE II. Calculated Raman and ir-active modes. For a more detailed description of these modes, including polarization-vector patterns, we refer to Ref. 13.

Raman active modes (cm ⁻¹)			Infrared active modes (cm ⁻¹)					
A _g	B _{2g}	B _{3g}	B _{1u}		B _{2u}		B _{3u}	
			TO	LO	TO	LO	TO	LO
116	73	92	95	122	103	104	81	81
157	142	137	155	184	127	140	121	121
355	356	412	199	209	191	193	168	171
378	429	496	312	312	350	358	198	204
508	564	544	363	417	368	449	356	367
			509	529	545	546	369	416
			573	577	573	573	565	565

through an enhancement of the dynamical screening in the direction normal to these planes, by assuming for YBa₂Cu₃O_{7-x} a large oxygen polarizability not only along Cu-O directions (the same as that along the Ti-O direction in BaTiO₃) but also in the direction normal to the O(II)-O(III) planes. With this modification the model gave, without any further adjustment, quite close agreement with the experimental ir and Raman data for YBa₂Cu₃O_{7-x}, and allowed the classification of the observed modes according to the symmetries of the calculated eigenvectors.^{12,13} The calculated ir and Raman frequencies and their classification are given in Table II; for a comparison with the experimental data, we refer to Ref. 13. So far, we have made no attempt to fine tune the model parameters any further in order to fit the experimental data as close as possible, since we wanted to see how well a model, based on these rather stringent assumptions would perform. Moreover, a procedure of fitting to the experimental data would certainly require that allowances be made for the changes in the potentials due to the different environments of otherwise equal partners, and for deviations from two-body central potentials. Thus, a fine-tuning only makes sense when additional data

about the measured dispersion curves will be available. At present, we are predicting these curves from our first approximation.

Results. Figure 1 shows the calculated dispersion curves in the three main symmetry directions. It can be seen that our dispersion curves are stable in all three directions. This is far from trivial since the YBa₂Cu₃O_{7-x} structure tends to give rise to phonon instabilities, with the result that there are only very narrow windows in the parameter space of these potentials, which lead to stable dispersion curves throughout the Brillouin zone. The curves shown here are stable throughout the entire Brillouin zone, not only in the directions shown in Fig. 1. In order to achieve this stability, a slight tuning of the potential parameters was required. Especially the low-frequency branches are very sensitive to small changes of the parameters of the potentials and since experimental data in the low-frequency range below 120 cm⁻¹ are not available, our predictions of these branches may be less reliable than those for the other branches. Even for the latter we have to admit some uncertainty, in particular, as far as the dispersion of the highest branches in the (0,1,0) direction is concerned, because they depend sensitively on the particular choice of the electronic polarizability of the oxygen. Using this model, we have further

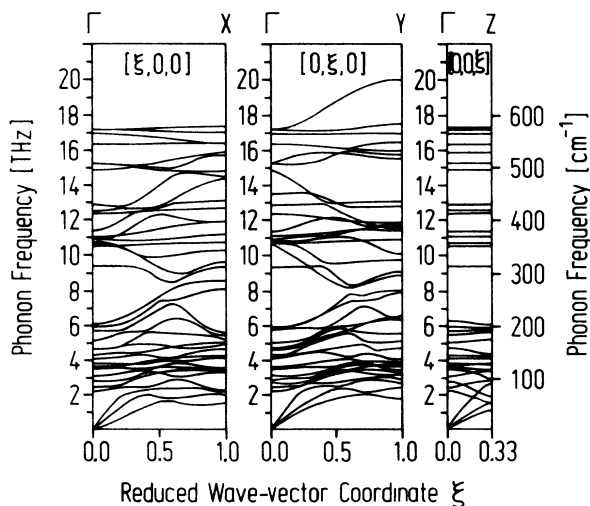


FIG. 1. Calculated phonon dispersion curves in the main symmetry directions $[\xi, 0, 0]$, $[\xi, \xi, 0]$, and $[0, 0, \xi]$ of the Brillouin zone.

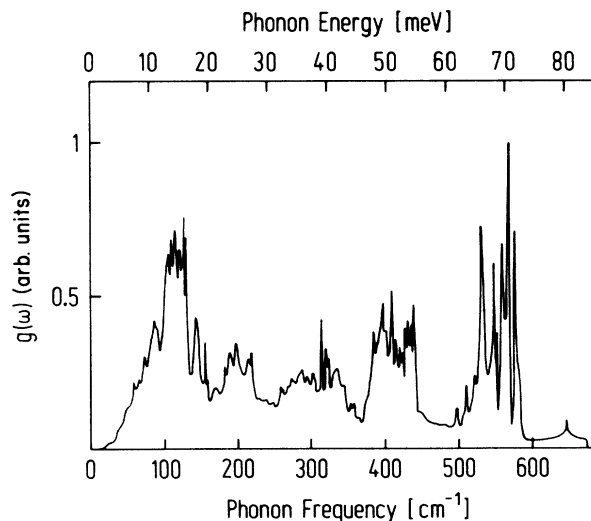


FIG. 2. Calculated one-phonon density of states $g(\omega)$.

calculated the one-phonon density of states given in Fig. 2. This density compared quite well with the data obtained from inelastic neutron-scattering measurements on powder samples.¹⁴ Comparison with these experimental data indicates that the first peak might have to be shifted by about 10% to higher energies. Similar unpublished data by Renker, Gompf, Gerling, and Ewert¹⁵ lead to the same conclusions. In addition, the data of the latter group deviate from our calculations in the relative intensities. These relative intensities are, however, not expected to be equal since the experimental data yield the amplitude weighted one-phonon densities while we present in Fig. 2 the proper one-phonon density of states.

Our calculations yield not only the phonon frequencies at the center of the Brillouin zone but also the phonon dispersion curves and the one-phonon density of states; it can, therefore, serve as a guide for further experimental investigations and as a tool for the investigation of the role phonons may play for the high transition temperatures of $\text{YBa}_2\text{Cu}_3\text{O}_{7-x}$. Our approach of carrying over two-particle potentials from metal oxides with sodium chloride and perovskite structures to $\text{YBa}_2\text{Cu}_3\text{O}_{7-x}$, leading to results in reasonable agreement with the available experimental data, helps to answer the question of whether there is something special about the phonons, and in consequence, about the interactions in $\text{YBa}_2\text{Cu}_3\text{O}_{7-x}$ as compared to perovskites. On the basis of the present results, our conclusion is that there seem to be no drastic differences in the interactions. The $\text{YBa}_2\text{Cu}_3\text{O}_{7-x}$ compound has high-lying modes which are essentially localized oxygen vibrations and it tends to exhibit instabilities, similar to those observed in perovskites. Finally, the high values for the electronic polarizabilities in our model point to a very strong electron-phonon interaction in these compounds. It could well be that the combination of these three properties, namely, (1) a tendency to instabilities

similar to those observed in perovskites, (2) high-frequency modes which are essentially oxygen vibrations, and (3) extremely large polarizabilities, lead to a strong phonon contribution to the high values of the superconducting transition temperature of these compounds.

Comparing our calculations with those presented in Ref. 16 we consider ours to be a more physical approach, giving rise to a deeper and more realistic description than a treatment with valence force field parameters which is, for the present class of materials, less appropriate than for covalent crystals. Moreover, an approach such as that of Ref. 16 has the additional disadvantage that the number of fit parameters nearly outnumbers the available experimental data. Our approach also goes beyond the calculations of Stavola *et al.*¹⁷ in which a simple force-constant model is fitted to the optical data measured at the zone center, instead of dealing with interaction potentials in the framework of a shell model. Both calculations have, however, in common that the force constants of Ref. 17 can be thought to arise from two-body central potentials and in consequence correspond to the effective short-range part of our model. Finally, it should be pointed out that our calculation yields a density-of-states function which shows a close resemblance with the results obtained by Weber and Mattheiss¹⁸ on the basis of a short-range force-constant model in which the renormalization due to the conduction electrons is properly taken into account in the framework of the nonorthogonal tight-binding theory.¹⁹

One of us (J.P.) was supported by a grant from the Deutsche Forschungsgemeinschaft. The work of another one of us (F.W.dW.) was supported by the National Science Foundation through Grant No. DMR-8505747 and by the Robert A. Welch Foundation through Grant No. F-433. A NATO grant for international collaboration is gratefully acknowledged.

*Permanent address: Universität Regensburg, D-8400 Regensburg, Federal Republic of Germany.

¹J. G. Bednorz and K. A. Müller, *Z. Phys. B* **64**, 189 (1986).

²M. K. Wu, J. R. Ashburn, C. J. Torng, P. H. Hor, R. L. Meng, L. Gao, Z. J. Huang, Y. Q. Wang, and C. W. Chu, *Phys. Rev. Lett.* **58**, 908 (1987).

³N. Lehner, H. Rauh, K. Strobel, R. Geick, G. Heger, J. Bouillot, B. Renker, M. Rousseau, and W. G. Stirling, *J. Phys. C* **15**, 6545 (1982).

⁴W. Kress, F. W. de Wette, A. D. Kulkarni, and U. Schröder, *Phys. Rev. B* **35**, 5783 (1987).

⁵R. Reiger, J. Prade, U. Schröder, W. Kress, and F. W. de Wette, *Surf. Sci.* **189/190**, 704 (1987); R. Reiger, J. Prade, U. Schröder, F. W. de Wette, and W. Kress, *J. Electron. Spectrosc. Relat. Phenom.* **44**, 403 (1987).

⁶J. Prade, A. D. Kulkarni, F. W. de Wette, W. Kress, M. Cardona, R. Reiger, and U. Schröder, *Solid State Commun.* **64**, 1267 (1987).

⁷B. Jannot, C. Escribe-Filippini, and J. Bouillot, *J. Phys. C* **17**, 1329 (1984).

⁸J. Bouillot, C. Escribe, W. J. Fitzgerald, and L. Gnininvi, *Solid State Commun.* **30**, 521 (1979).

⁹W. Reichardt, V. Wagner, and W. Kress, *J. Phys. C* **8**, 3955 (1975).

¹⁰K. H. Rieder, R. Migoni, and B. Renker, *Phys. Rev. B* **12**, 3374 (1975).

¹¹F. Beech, S. Miraglia, A. Santoro, and R. S. Roth, *Phys. Rev. B* **35**, 8778 (1987).

¹²C. Thomsen, M. Cardona, W. Kress, R. Liu, L. Genzel, M. Bauer, E. Schönherr, and U. Schröder, *Solid State Commun.* **65**, 1139 (1988).

¹³R. Liu, C. Thomsen, W. Kress, M. Cardona, B. Gegenheimer, F. W. de Wette, J. Prade, A. D. Kulkarni, and U. Schröder, *Phys. Rev. B* **37**, 7971 (1988).

¹⁴J. J. Rhyne, D. A. Neumann, J. A. Gotaas, F. Beech, L. Toth, S. Lawrence, S. Wolf, M. Osofsky, and D. U. Gubser, *Phys. Rev. B* **36**, 2294 (1987).

¹⁵B. Renker, F. Gompf, E. Gerling, and D. Ewert (private communication).

¹⁶F. E. Bates and J. E. Eldridge, *Solid State Commun.* **64**, 1435 (1987).

¹⁷M. Stavola, D. M. Krol, W. Weber, S. A. Sunshine, A. Jayaraman, G. A. Kourouklis, R. J. Cava, and E. A. Rietmann, *Phys. Rev. B* **36**, 850 (1987).

¹⁸W. Weber and L. F. Mattheiss, *Phys. Rev. B* **37**, 599 (1988).

¹⁹C. M. Varma and W. Weber, *Phys. Rev. B* **19**, 6142 (1979).